Cell Metabolism, Volume *34*

Supplemental information

STING orchestrates the crosstalk between polyunsaturated fatty acid metabolism and inflammatory responses

Isabelle K. Vila, Hanane Chamma, Alizée Steer, Mathilde Saccas, Clara Taffoni, Evgenia Turtoi, Line S. Reinert, Saqib Hussain, Johanna Marines, Lei Jin, Xavier Bonnefont, Mathieu Hubert, Olivier Schwartz, Soren R. Paludan, Gaetan Van Simaeys, Gilles Doumont, Bijan Sobhian, Dimitrios Vlachakis, Andrei Turtoi, and Nadine Laguette

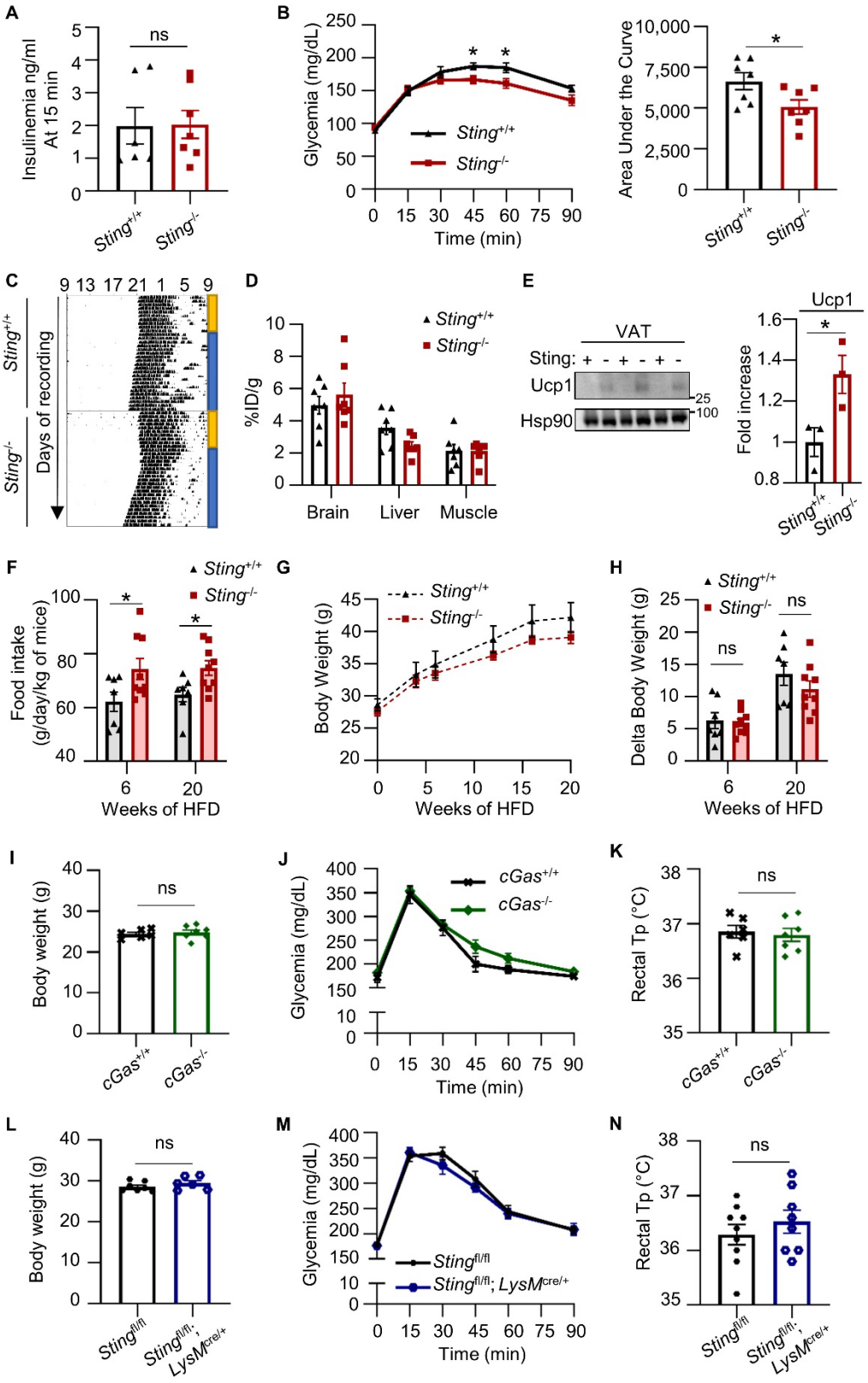

Figure S1: STING Deficiency Leads to Global Metabolic Improvement Independently of its Canonical Function

(A) Insulinemia was measured 15 min after the injection of glucose during a GTT test in *Sting*$^{+/+}$ (n=6) and *Sting*$^{-/-}$ (n=7) mice.

(B) Pyruvate tolerance test (PTT) was performed in *Sting*$^{+/+}$ (n=7) and *Sting*$^{-/-}$ (n=7) mice; Left panel: glycemia over time after pyruvate bolus injection; Right panel: AUC of PTT.

(C) Representative actograms of running-wheel activity from *Sting*$^{+/+}$ (n=11) and *Sting*$^{-/-}$ (n=10) mice, under a regular light-dark cycle (Yellow) or constant darkness (Blue).

(D) Biodistribution (%ID/g) of [18F]-FDG in *Sting*$^{+/+}$ (n=7) and *Sting*$^{-/-}$ (n=7) mice; The %ID/g is defined as percentage of total injection dose (ID) per gram tissue weight.

(E) Ucp1 protein levels were measured in the visceral adipose tissue (VAT) from *Sting*$^{+/+}$ (n=3) and *Sting*$^{-/-}$ (n=3) mice.

(F) Body weight over time in *Sting*$^{+/+}$ (n=7) and *Sting*$^{-/-}$ (n=9) mice under high fat diet (HFD-60% fat).

(G) Delta body weight calculated at 6 and 20 weeks of HFD in *Sting*$^{+/+}$ (n=7) and *Sting*$^{-/-}$ (n=9) mice.

(H) Food intake in *Sting*$^{+/+}$ (n=7) and *Sting*$^{-/-}$ (n=9) mice under HFD for 6 and 20 weeks.

(I) Body weight of *cGas*$^{+/+}$ (n=6) and *cGas*$^{-/-}$ (n=7) mice fed on normal chow diet was measured at 8 weeks age.

(J) Glucose tolerance test (GTT) was performed in *cGas*$^{+/+}$ (n=5) and *cGas*$^{-/-}$ (n=5) mice.

(K) Rectal temperature was measured in *cGas*$^{+/+}$ (n=6) and *cGas*$^{-/-}$ (n=7) mice.

(L) Body weight of *Sting*$^{fl/fl}$ (n=7) and *Sting*$^{fl/fl}$; *LysM*$^{cre/+}$ (n=8) mice fed on normal chow diet was measured at 8 weeks of age.

(M) GTT was performed in *Sting*$^{fl/fl}$ (n=7) and *Sting*$^{fl/fl}$; *LysM*$^{cre/+}$ (n=6) mice.

(N) Rectal temperature of *Sting*$^{fl/fl}$ (n=9) and *Sting*$^{fl/fl}$; *LysM*$^{cre/+}$ (n=8) mice was measured. Graphs present means ± SEM. P-values were determined by Student's t-test. *: P< 0.05, **: P< 0.01, ***: P< 0.001.

Related to Figure 1.

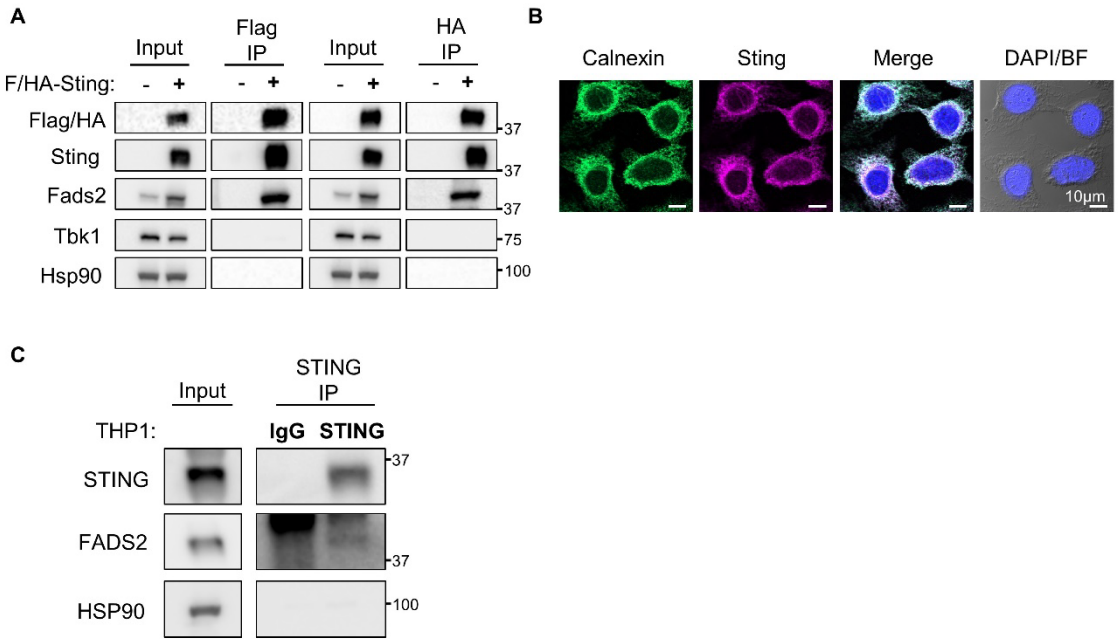

Figure S2: STING Interacts with FADS2

(A) WB analysis of Inputs and Flag- or HA-immunoprecipitated Sting in MEF$^{Sting-/-}$ stably expressing F/HA-Sting.

(B) Immunofluorescence analysis of MEF$^{Sting-/-}$ stably expressing F/HA-Sting using anti-Calnexin and anti-HA antibodies and DAPI nuclear staining. BF: Bright-Field.

(C) WB analysis of Inputs and STING-specific immunoprecipitation in THP-1 human cells.

Graphs present means ± SEM. P-values were determined by Student's t-test. *: P< 0.05, **: P< 0.01, ***: P< 0.001.

Related to Figure 2 and Table 1.

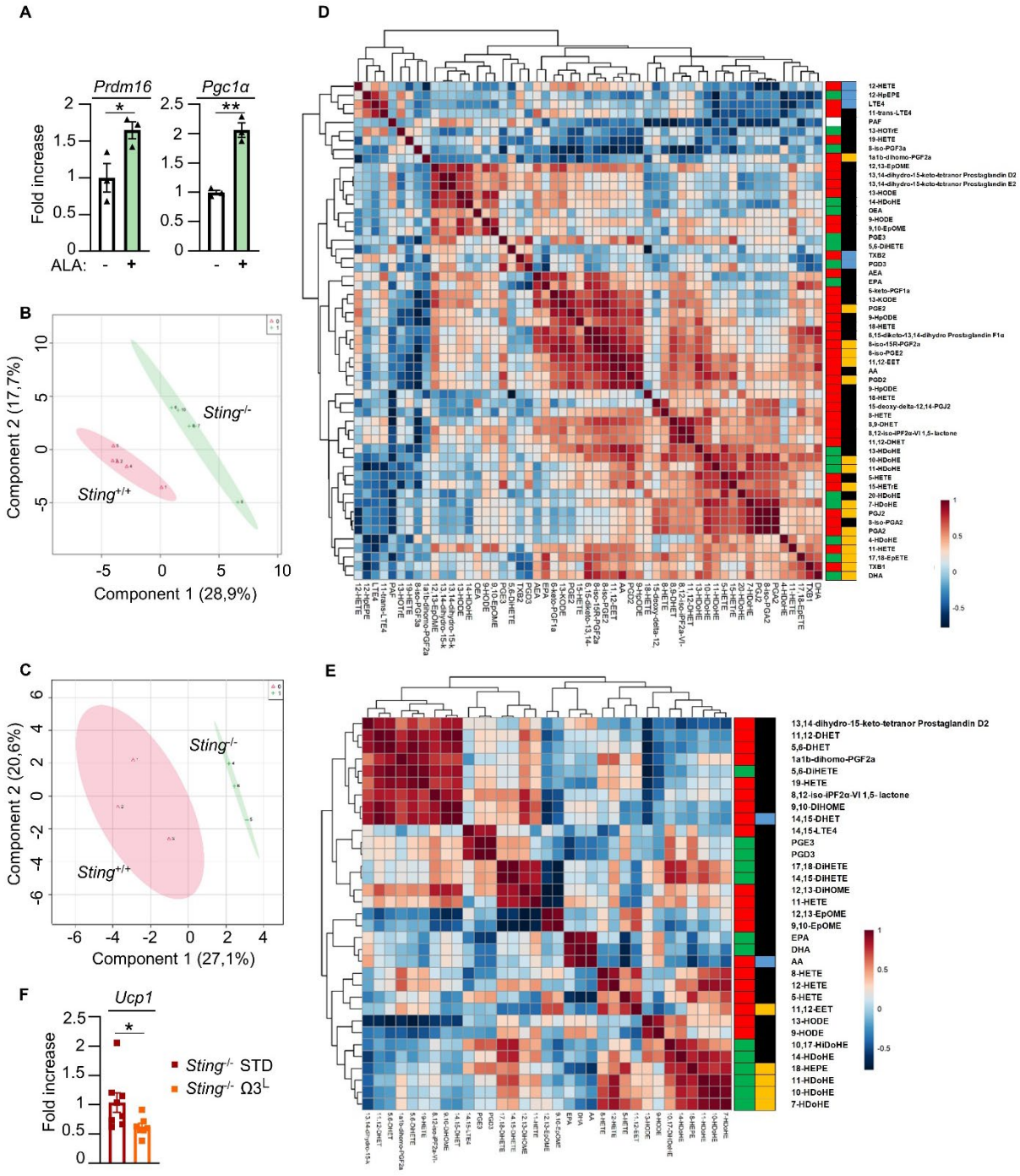

Figure S3: STING Modulates Polyunsaturated Fatty Acids Pools

(A) *Pgc1α* and *Prdm16* mRNA levels in 293T cells treated or not with ALA for 24 h (n=3).

(B) Partial least squares discriminant analysis (PLS-DA) of liver samples from *Sting*$^{+/+}$ (pink) and *Sting*$^{-/-}$ (green) mice in which PUFAs and derivatives were measured by LC-MS (n=5 mice per group).

(C) As in B, except that VAT samples were used (n=3 mice per group).

(D) Correlation matrix showing groups of metabolites that are positively (red) or negatively (blue) correlated in terms of quantitative modulation between liver samples from (B). Right

hand side color coding: (first scale) metabolites derived from Ω-6 or Ω-3 are in red or green respectively; (second scale) metabolites increased or decreased by more than 30% in *Sting*$^{-/-}$ as compared to *Sting*$^{+/+}$, are in yellow or blue respectively.

(E) As in D, except that VAT samples from (C) were analyzed.

(F) *Ucp1* mRNA levels were analyzed from the VAT of *Sting*$^{-/-}$ mice under STD or Ω3^{L} diet.

Graphs present means ± SEM. P-values were determined by Student's t-test. *: P< 0.05, **: P< 0.01, ***: P< 0.001.

Related to Figure 3.

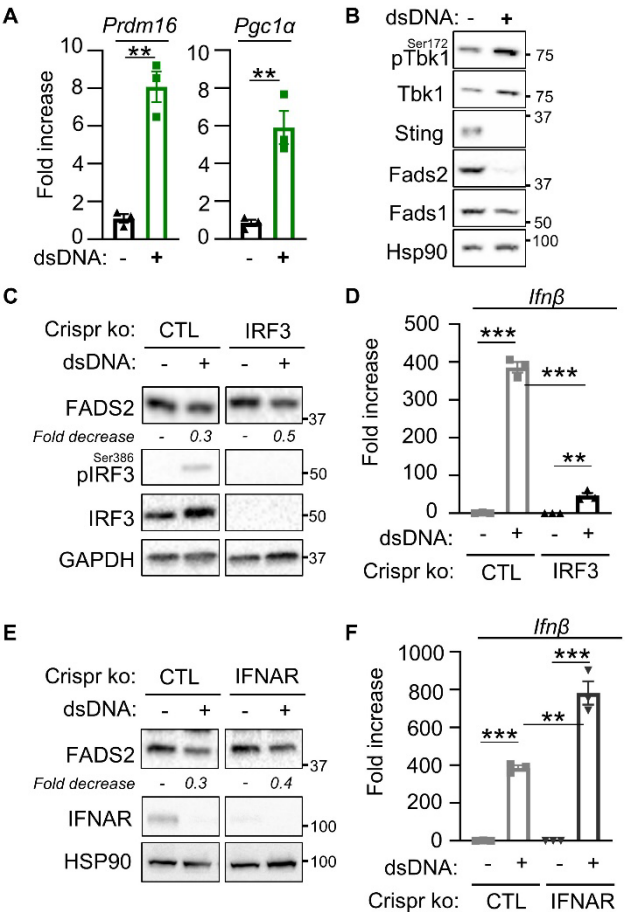

Figure S4: STING activation leads to increased FADS2-dependent Desaturation Activity

(A) *Prdm16* and *Pgc1α* mRNA levels in 293T cells transfected or not with dsDNA for 24 h (n=3).

(B) WCE from MEF stimulated or not for 6 h with dsDNA were analyzed by WB using indicated antibodies.

(C) WCE from control (CTL) or IRF3 knockout T98G cell lines, stimulated or not for 6 h with dsDNA, were analyzed by WB using indicated antibodies.

(D) *Ifnβ* mRNA levels from samples treated as in (B) were analyzed by RT-qPCR. Representative experiment, n=3.

(E) WCE from control (CTL) or IFNAR1 knockout T98G cell lines stimulated or not for 6 h with dsDNA were analyzed by WB using indicated antibodies.

(F) *Ifnβ* mRNA levels from samples treated as in (D) were analyzed by RT-qPCR. Graph presents mean fold induction ± SEM, as compared to unstimulated control cells. Representative experiment, n=3.

All graph present means ± SEM. P-values were determined by Student's t-test. **P: < 0.01, ***P: < 0.001.

Related to Figure 4.

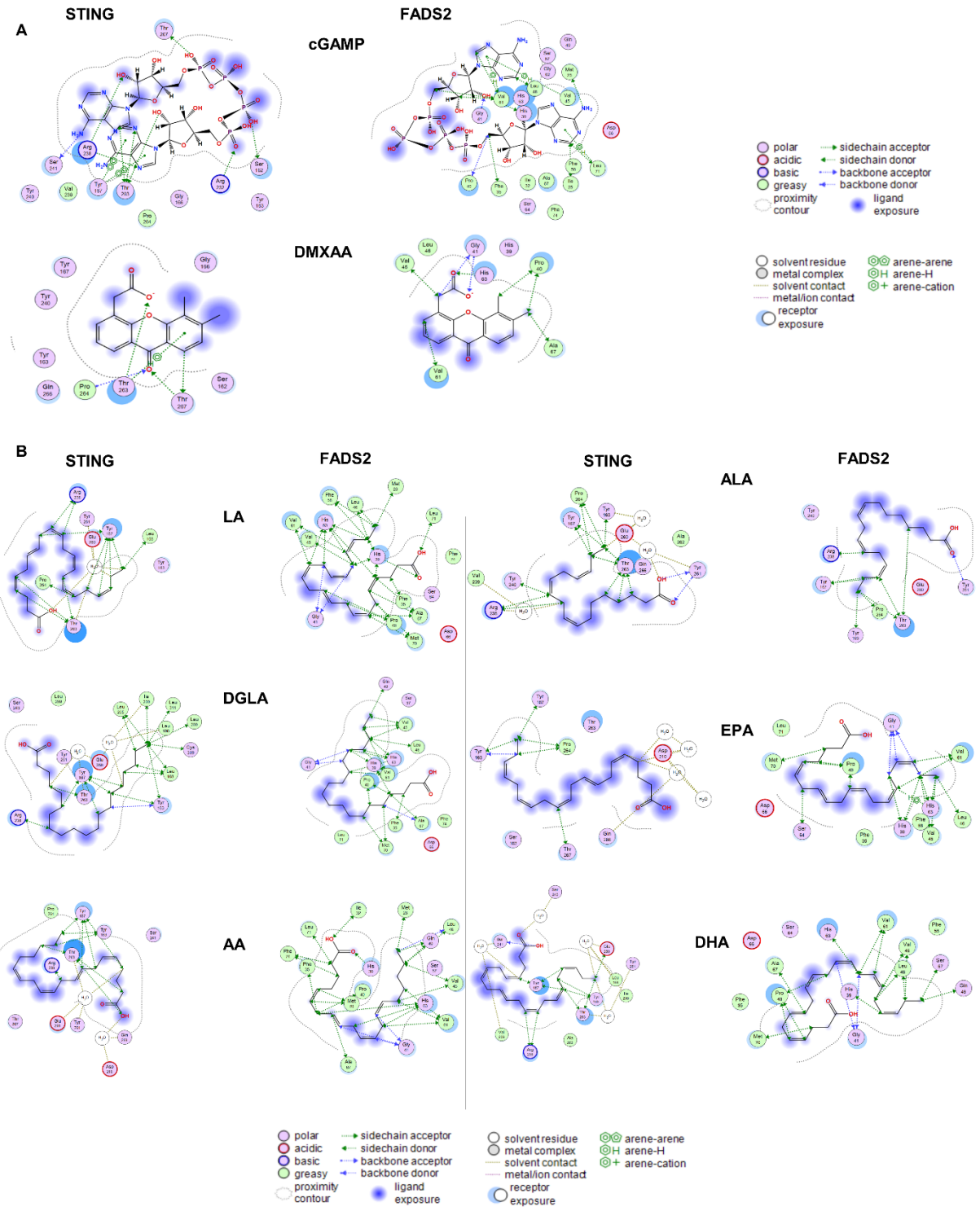

Figure S5: PUFAs interact with the cGAMP-binding domain of STING.

(A) 2D molecular interaction maps for cGAMP and DMXAA docked into STING (left column) and FADS2 (right column).

(B) 2D molecular interaction maps for the 6 PUFAs docked into STING (left column) and FADS2 (right column). LA: linoleic acid, DGLA: Dihomo-γ -linolenic acid, AA: arachidonic acid, ALA: α-linolenic acid, EPA: eicosapentaenoic acid, DHA: docosahexaenoic acid.

Related to Figure 5.

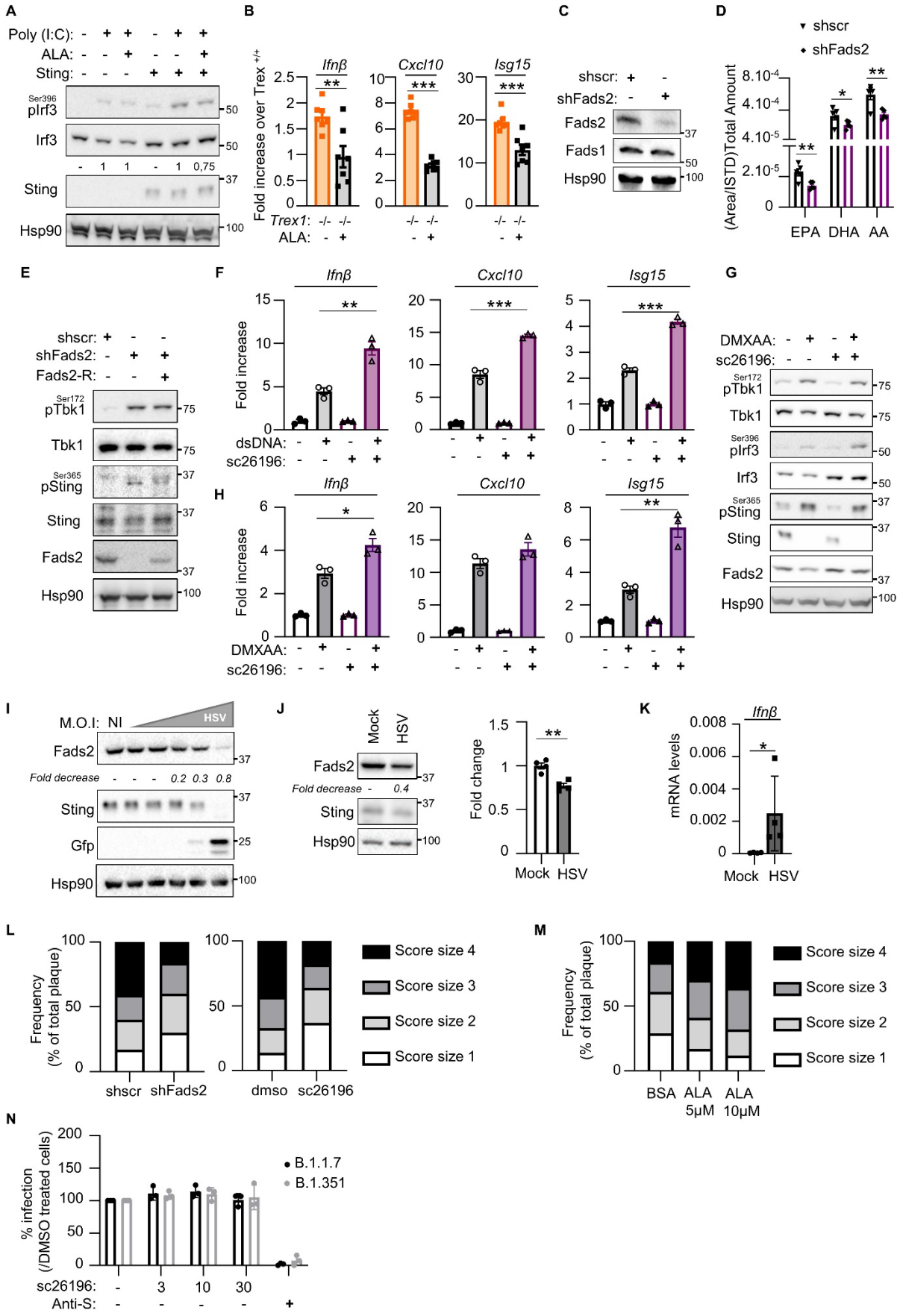

Figure S6: PUFAs inhibit STING activation.

(A) WCE from WT-MEFs and MEF$^{Sting-/-}$ treated or not with 2 µg of poly(I:C) for 6 h in the presence or absence of 50 µM ALA, were analyzed by WB using the indicated antibodies.
(B) MEF$^{Trex1-/-}$ were treated or not with 50 µM ALA for 18 h prior to analysis of *Ifnβ*, *Cxcl10* and *Isg15* mRNA levels.
(C) PUFAs measured in cells expressing Scramble (scr) or Fads2-targeting shRNAs using LC-MS. Graph presents indicated PUFAs.
(D) WCE from MEF stably expressing scrambled (shscr) or Fads2-targeting (shFads2) shRNAs were analyzed by WB using the indicated antibodies.
(E) WCE from MEF stably expressing shscr or shFads2, re-expressing or not a shFads2-resistant Fads2 allele, were analyzed by WB using the indicated antibodies.
(F) *Ifnβ*, *Cxcl10* and *Isg15* mRNA levels were analyzed from WT-MEF transfected with dsDNA for 6 h in the presence or not of 4 µM of the sc26196 Fads2 inhibitor.
(G) WCE of cells treated as in E were analyzed by WB using the indicated antibodies.
(H) *Ifnβ*, *Cxcl10* and *Isg15* mRNA levels were analyzed from WT-MEF treated with DMXAA for 6h in the presence or not of 4 µM of the sc26196 Fads2 inhibitor.
(I) WCE from WT-MEFs, infected or not for 16 h with HSV-KOS64, were analyzed by WB using indicated antibodies. Multiplicity of infection (MOI) scale was from $1.5x10^{-4}$ to 1.5.
(J) Left: Representative mice brain samples infected or not for 5 days with the McKrae HSV-1 strain were analyzed by WB using indicated antibodies. Right: Quantification of Fads2 protein levels in mice brain extracts following 5 days of infection or not with McKrae HSV1 (n=4).
(K) *Ifnβ* mRNA levels from samples in (I).
(L) Quantification of the size of plaques following infection by HSV-1 as performed in Figure 6I are expressed as a percentage of total plaque number.
(M) Quantification of the size of plaques following infection by HSV-1 as performed in Figure 6J are expressed as a percentage of total plaque number.
(N) Caco-2/TC7 cells were infected with B.1.1.7 or B.1.351 SARS-CoV2 strains prior to quantification of the % infected cells, in the presence of the indicated doses of the sc26196 Fads2 inhibitor. Anti-S: An anti-SARS-CoV-2 Spike neutralizing antibody inhibits viral replication and was used as a positive control. Results are normalized to the no drug condition, n=3.
All graph present means ± SEM. P-values were determined by Student's t-test. ns: not significant. *: $P < 0.05$, **P: < 0.01, ***P: < 0.001.
Related to Figure 6.

Supplementary Tables:

Table S1. Interaction energies of the docked cGAMP, DMXAA and the 6 PUFAs on STING and FADS2. Energies are in Kcal/mol. Related to Figure 4 and S4.

	STING	FADS2
cGAMP	-34.925	-7.269
DMXAA	-24.400	-51.661
linoleic acid (LA)	-39.483	-57.098
dihomo-γ-linolenic acid (DGLA)	-13.064	-47.331
arachidonic acid (AA)	-42.827	-58.912
α-linolenic acid (ALA)	-43.658	-38.473
eicosapentaenoic acid (EPA)	-24.926	-41.078
docosahexaenoic acid (DHA)	-53.608	-57.339

Table S2. Composition of Standard (STD) and Low Omega3 ($\Omega 3^{L}$) diets. Related to Key Resources Table.

OMEGA STD diet & OMEGA3 ^{L} diet Composition		
FORMULA INGREDIENTS (g/kg)	**STD diet**	**$\Omega 3^{L}$ diet**
soybean oil	10	0
oil pepin from grape	10	20
cocoa butter	20	30
Calculated Nutritional Values (g/100g)	**STD diet**	**$\Omega 3^{L}$ diet**
Energy from proteins	16.67	16.67
Energy from lipids	17.38	17.38
Energy from NFE	65.96	65.95
Energy from sugar	14.46	14.45
Energy from starch	50.05	50.05
Calculated Nutritional Values (mg/Kg)	**STD diet**	**$\Omega 3^{L}$ diet**
Saturated fatty acids (SFAs)	26 305.00	28 006.00
Unsaturated fatty acids (UFAs)	40 601.80	39 175.20
Monounsaturated fatty acids (MUFAs)	23 588.10	22 439.40
Polyunsaturated fatty acids (PUFAs)	17 013.70	16 735.80
Total omega 3 fatty acids	**1 178.70**	**385.80**

C18:3 Alpha-linolenic acid (ALA)	1 178.70	385.80
C20:5 EPA	0.00	0.00
C22:5 DPA	0.00	0.00
C22:6 DHA	0.00	0.00
Total omega 6 fatty acids	**15 835.00**	**16 350.00**
C18:2 Linoleic acid (LA)	15 325.00	16 010.00
Ratio omega 6/3	**13.4**	**42.4**

Table S3. Oligonucleotides for gene expression analysis and Guide RNAs for the CRISPR-Cas9 system. Related to Key Resources Table.

Oligonucleotides	**Forward primer**	**Reverse primer**
GAPDH	CTGGCGTCTTCACCACCATGG	CATCACGCCACAGTTTCCCGG
IFNβ	GAATGGGAGGCTTGAATACTGCCT	TAGCAAAGATGTTCTGGAGCATCTC
Gapdh	TTCACCACCATGGAGAAGGC	GGCATCGACTGTGGTCATGA
Ifnβ	CTGCGTTCCTGCTGTGCTTCTCCA	TTCTCCGTCATCTCCATAGGGATC
Cxcl10	ATGACGGGCCAGTGAGAATG	TCAACACGTGGGCAGGATAG
Isg15	GTGCTCCAGGACGGTCTTAC	CTCGCTGCAGTTCTGTACCA
Hsp90	GTCCGCCGTGTGTTCATCAT	GCACTTCTTGACGATGTTCTTGC
Tnfα	CTGTAGCCCACGTCGTAGC	TTGAGATCCATGCCGTTG
Il-6	GACTTCCATCCAGTTGCCTTCT	TCCTCTCCGGACTTGTGAAGTA
Ucp1	CCTGCCTCTCTCGGAAACAA	TGTAGGCTGCCCAATGAACA
Pgc1α	AAAGGATGCGCTCTCGTTCA	GGAATATGGTGATCGGGAACA
Prdm16	CAGCACGGTGAAGCCATTC	GCGTCGATCCGCTTGTG
Cidea	TGCTCTTCTGTATCGCCCAGT	GCCGTGTTAAGGAATCTGCTG
Dio2	GCTTACGGGGTAGCCTTTGA	CCAGCCAACTTCGGACTTCT
Guide RNAs for the CRISPR-Cas9 system	**Guide 1**	**Guide 2**
Control	CACCGAGCACGTAATGTCCGTGGAT	AAACATCCACGGACATTACGTGCTC
IRF3	CACCGAGCTGACACTCACCTTCCCC	AAACGGGGAAGGTGAGTGTCAGCTC

IFNAR1	CACCGAAGCAGCACTACTTAC GTCA	AAACTGACGTAAGTAGT GCTGCTTC